arXiv:1109.3039v2 [nucl-th] 11 Jan 2012

Rise of azimuthal anisotropies as a signature of the Quark-Gluon-Plasma in relativistic heavy-ion collisions

V. P. Konchakovski,[1,2] E. L. Bratkovskaya,[3,4] W. Cassing,[1] V. D Toneev,[4,5] and V. Voronyuk[2,4,5]

[1]*Institute for Theoretical Physics, University of Giessen, Giessen, Germany*
[2]*Bogolyubov Institute for Theoretical Physics, Kiev, Ukraine*
[3]*Institute for Theoretical Physics, University of Frankfurt, Frankfurt, Germany*
[4]*Frankfurt Institute for Advanced Studies, Frankfurt, Germany*
[5]*Joint Institute for Nuclear Research, Dubna, Russia*

The azimuthal anisotropies of the collective transverse flow of hadrons are investigated in a large range of heavy-ion collision energy within the Parton-Hadron-String Dynamics (PHSD) microscopic transport approach which incorporates explicit partonic degrees of freedom in terms of strongly interacting quasiparticles (quarks and gluons) in line with an equation-of-state from lattice QCD as well as dynamical hadronization and hadronic dynamics in the final reaction phase. The experimentally observed increase of the elliptic flow v_2 with bombarding energy is successfully described in terms of the PHSD approach in contrast to a variety of other kinetic models based on hadronic interactions. The analysis of higher-order harmonics v_3 and v_4 shows a similar tendency of growing deviations between partonic and purely hadronic models with increasing bombarding energy. This signals that the excitation functions of azimuthal anisotropies provide a sensitive probe for the underling degrees of freedom excited in heavy-ion collisions.

PACS numbers: 25.75.-q, 25.75.Ag

Introduction. A few decades of experimental studies at the Schwerionen-Synchrotron (SIS), the Alternating Gradient Synchroton (AGS) and the Super Proton Synchroton (SPS) have shown that the physics of nuclear collisions at moderate relativistic energies is dominated by the nonequilibrium dynamics of hadronic resonance matter, *i.e.* the confined phase of QCD. The body of data extends and builds up the knowledge gained about dense hadronic matter, in particular, at the SPS/CERN. The SPS heavy-ion data have shown several signatures that hinted at the onset of a quark-gluon plasma (QGP) formation [1, 2]. With the Relativistic Heavy Ion Collider (RHIC) the center-of-mass energy could be increased by a factor of 10 relative to the SPS, and the experiments at RHIC assured that a new form of matter – well above the deconfinement transition point – was created in the laboratory.

Indeed, the discovery of a large azimuthal anisotropic flow of hadrons at RHIC provides a conclusive evidence for the creation of dense partonic matter in ultra-relativistic nucleus-nucleus collisions. The strongly interacting medium in the collision zone can be expected to achieve a local equilibrium and exhibit an approximately hydrodynamic flow [3–5]. The momentum anisotropy is generated due to pressure gradients in a collective expansion of an initial geometry of an "almond-shaped" collision zone produced in noncentral collisions [3, 4]. The pressure gradients translate early stage coordinate space asymmetry to final-state momentum space anisotropy [6]. The picture thus emerges that the medium created in ultra-relativistic collisions for a couple of fm/c interacts more strongly than hadron resonance matter and exhibits collective properties that resemble those of a liquid of a very low shear viscosity η to the entropy density s ratio, η/s, close to a nearly perfect fluid [7–9].

An experimental manifestation of this collective flow is the anisotropic emission of particles in the plane transverse to the beam direction. A quark number scaling of the elliptic flow proposed in Ref. [10] was observed at RHIC for a broad range of particle species, collision centralities, and transverse kinetic energy, presumably interpreted as due to the development of substantial collectivity in the early partonic phase [11].

It was shown that higher-order anisotropy harmonics, in particular the hexadecupole moment v_4, can provide a more sensitive constraint on the magnitude of η/s and the freeze-out dynamics, and the ratio $v_4/(v_2)^2$ might indicate whether a full local equilibrium is achieved in the QGP [12]. Recently, the importance of the triangular flow v_3, which originates from fluctuations in the initial collision geometry, has been pointed out [13, 14]. The participant triangularity characterizes the triangular anisotropy of the initial nuclear overlap geometry and arises from event-by-event fluctuations in the participant-nucleon collision points and corresponds to a large third Fourier component in two-particle azimuthal correlations at large pseudo-rapidity separation $\Delta\eta$. This fact suggests a significant contribution of the triangular flow to the ridge phenomenon and broad away-side structures observed in the RHIC data [13].

A large number of anisotropic flow measurements have been performed by many experimental groups at SIS, AGS, SPS and RHIC energies over the past 20 years. Very recently the azimuthal asymmetry has also been measured at the Large Hadron Collider (LHC) at CERN [15]. The Beam Energy Scan (BES) program proposed at RHIC [16] covers the energy interval from $\sqrt{s_{NN}} = 200$ GeV, where partonic degrees of freedom (DOF) play a decisive role, down to the AGS energy $\sqrt{s_{NN}} \approx 5$ GeV, where most experimental data can be

described successfully in terms of hadronic DOF Lowering the collision energy and studying the energy dependence of an anisotropic flow allows one to search for the onset of the transition to a phase with partonic DOF at an early stage of the collision as well as possibly identify the location of the expected critical end-point that terminates the first order phase transition at high quark-chemical potential [11, 17].

This work aims to study excitation functions for different harmonics of the charged particle anisotropy in momentum space in a wide collision energy range, i.e. from the AGS to the top RHIC energy regime. We want to clarify how the interplay of quark and hadron DOF is changed with increasing bombarding energy. In this study we investigate the excitation function of different flow coefficients. Our analysis of the STAR/PHENIX RHIC data – based on recent results of the BES program – will be performed within the PHSD transport approach [18] that includes explicit partonic DOF as well as a dynamic hadronization scheme for the transition from partonic to hadronic DOF and vice versa.

The PHSD approach. The dynamics of partons, hadrons and strings in relativistic nucleus-nucleus collisions is analyzed here within the Parton-Hadron-String Dynamics approach [18]. In this transport approach the partonic dynamics is based on Kadanoff-Baym equations for Green functions with self-energies from the Dynamical QuasiParticle Model (DQPM) [19, 20] which describes QCD properties in terms of "resummed" single-particle Green functions. In Ref. [21], the actual three DQPM parameters for the temperature-dependent effective coupling were fitted to the recent lattice QCD results of Ref. [22]. The latter lead to a critical temperature $T_c \approx 160$ MeV which corresponds to a critical energy density of $\epsilon_c \approx 0.5$ GeV/fm^3. In PHSD the parton spectral functions ρ_j $(j = q, \bar{q}, g)$ are no longer δ-functions in the invariant mass squared as in conventional cascade or transport models but depend on the parton mass and width parameters which were fixed by fitting the lattice QCD results from Ref. [22]. We recall that the DQPM allows one to extract a potential energy density V_p from the space-like part of the energy-momentum tensor as a function of the scalar parton density ρ_s. Derivatives of V_p with respect to ρ_s then define a scalar mean-field potential $U_s(\rho_s)$ which enters into the equation of motion for the dynamic partonic quasiparticles. Furthermore, a two-body interaction strength can be extracted from the DQPM as well from the quasiparticle width in line with Ref. [9]. The transition from partonic to hadronic DOF (and vice versa) is described by covariant transition rates for the fusion of quark-antiquark pairs or three quarks (antiquarks), respectively, obeying flavor current-conservation, color neutrality as well as energy-momentum conservation [18, 21]. Since the dynamical quarks and antiquarks become very massive close to the phase transition, the formed resonant "prehadronic" color-dipole states ($q\bar{q}$ or qqq) are of high invariant mass, too, and sequentially decay to the ground-state meson and baryon octets increasing the total entropy.

On the hadronic side PHSD includes explicitly the baryon octet and decouplet, the 0^-- and 1^--meson nonets as well as selected higher resonances as in the Hadron-String-Dynamics (HSD) approach [23, 24]. Hadrons of higher masses (> 1.5 GeV in case of baryons and > 1.3 GeV for mesons) are treated as "strings" (color dipoles) that decay to the known (low-mass) hadrons, according to the JETSET algorithm [25]. Note that PHSD and HSD merge at low energy density, in particular below the critical energy density $\epsilon_c \approx 0.5$ GeV/fm^3.

The PHSD approach was applied to nucleus-nucleus collisions from $\sqrt{s_{NN}} \sim 5$ to 200 GeV in Refs. [18, 21] in order to explore the space-time regions of "partonic matter". It was found that even central collisions at the top-SPS energy of $\sqrt{s_{NN}} = 17.3$ GeV show a large fraction of nonpartonic, i.e., hadronic or stringlike matter, which can be viewed as a hadronic corona. This finding implies that neither hadronic nor only partonic "models" can be employed to extract physical conclusions in comparing model results with data. All these previous findings provide promising perspectives to use PHSD in the whole range from about $\sqrt{s_{NN}} = 5$ to 200 GeV for a systematic study of azimuthal asymmetries of hadrons produced in relativistic nucleus-nucleus collisions.

Calculational results and comparison to data. The anisotropy in the azimuthal angle ψ is usually characterized by the even order Fourier coefficients $v_n = \langle exp(\imath\, n(\psi - \Psi_{RP}))\rangle$, $n = 2, 4, ...$, since for a smooth angular profile the odd harmonics become equal to zero. As noted above, Ψ_{RP} is the azimuth of the reaction plane and the brackets denote averaging over particles and events. In particular, for the widely used second-order coefficient, denoted as an elliptic flow, we have

$$v_2 = \langle cos(2\psi - 2\Psi_{RP})\rangle = \left\langle \frac{p_x^2 - p_y^2}{p_x^2 + p_y^2} \right\rangle \ , \qquad (1)$$

where p_x and p_y are the x and y components of the particle momenta. This coefficient can be considered as a function of centrality, pseudorapidity η, and/or transverse momentum p_T. We note that the reaction plane in PHSD is given by the $(x - z)$ plane with the z axis in the beam direction. Integrated v_3 and v_4 coefficients are calculated by the two-particle correlation method in line with Ref. [26]:

$$\langle cos(n\psi_1 - n\psi_2))\rangle = \langle v_n^2\rangle + \delta_n \ , \qquad (2)$$

which is based on the assumption that nonflow contributions δ_n are small and account for event-by-event fluctuations of the event plane. In Fig. 1 the experimental v_2 excitation function in the transient energy range is compared to the results from the PHSD calculations; HSD model results are given as well for reference. We note that the centrality selection and acceptance are the same for the data and models.

We recall that the HSD model has been very successful in describing heavy-ion spectra and rapidity distributions from SIS to SPS energies. A detailed comparison

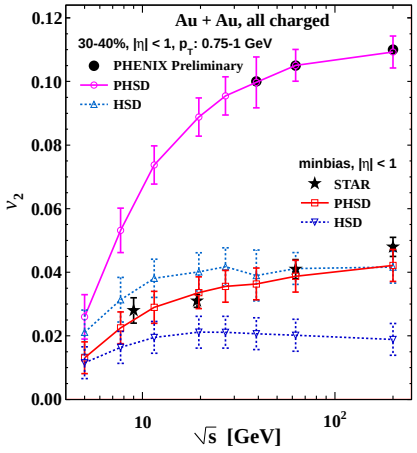


FIG. 1: Average elliptic flow v_2 of charged particles at midrapidity for two centrality selections calculated within the PHSD (solid curves) and HSD (dashed curves) approaches. The v_2 STAR data compilation for minimal bias collisions are taken from Ref. [27] (stars) and the preliminary PHENIX data [28] are plotted by solid circles.

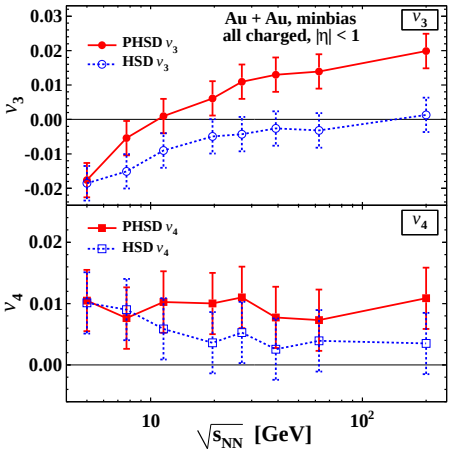


FIG. 2: Average anisotropic flows v_3 and v_4 of charged particles at mid-pseudorapidity for minimum bias collisions of $Au + Au$ calculated within the PHSD (solid lines) and HSD (dashed lines) models.

of HSD results with respect to a large experimental data set was reported in Ref. [29] for central Au+Au (Pb+Pb) collisions from AGS to top SPS energies. Indeed, as shown in Fig. 1 (dashed lines), HSD is in good agreement with experiment for both data sets at the lower edge ($\sqrt{s_{NN}} \sim 10$ GeV) but predicts an approximately energy-independent flow v_2 at larger energies and, therefore, does not match the experimental observations. This behavior is in quite close agreement with another independent hadronic model, the UrQMD (Ultra relativistic Quantum Molecular Dynamics) [30] (cf. with [27]).

From the above comparison one may conclude that the rise of v_2 with bombarding energy is not due to hadronic interactions and models with partonic DOF have to be addressed. Indeed, the PHSD approach incorporates the parton medium effects in line with a lQCD equation of state, as discussed above, and also includes a dynamic hadronization scheme based on covariant transition rates. It is seen from Fig. 1 that PHSD performs better: The elliptic flow v_2 from PHSD (solid curve) is fairly in line with the data from the STAR and PHENIX collaborations and clearly shows the growth of v_2 with the bombarding energy.

Since partonic DOF come into play, it is interesting to compare with another parton-hadron model, i.e. the AMPT (A Multi Phase Transport) model [31]. This model is based on a perturbative QCD description of partonic interactions, including the production of multiple minijet partons according to the number of binary initial collisions. As shown in Ref. [27], the AMPT model predicts an approximately constant v_2 with $\sqrt{s_{NN}}$ similar to the hadronic models HSD and UrQMD; however, the v_2 values match the experimental data at the top RHIC energy. This discrepancy is due to a pQCD description of the partonic phase in AMPT where the minijet partons are treated as massless and their potentials are disregarded when they undergo scattering. Note that PHSD and AMPT (with the additional strong hadron melting assumption in AMPT) practically give the same elliptic flow at the top RHIC energy of $\sqrt{s_{NN}} = 200$ GeV. We note that the PHSD model includes more realistic properties of dynamical quasiparticles especially in the vicinity of the critical energy density. Furthermore, the quark-gluon transport in PHSD naturally passes on to the (hadronic) HSD model at lower $\sqrt{s_{NN}}$.

In Fig. 2 we display the PHSD and HSD results for the anisotropic flows v_3 and v_4 of charged particles at midpseudorapidity for $Au + Au$ collisions from $\sqrt{s_{NN}} =$ 5 to 200 GeV. The triangular flow increases with $\sqrt{s_{NN}}$ having negative values for $\sqrt{s_{NN}} \lesssim 10$ GeV. The pure hadronic model HSD gives $v_3 \approx 0$ for $\sqrt{s_{NN}} \gtrsim$ (20-30) GeV. Accordingly, the results from PHSD (solid red lines) are systematically larger than those from HSD (dashed blue lines). Unfortunately, our statistics is not high enough to allow for more precise conclusions. The hexadecupole flow v_4 stays almost constant in the considered energy range; here PHSD gives slightly higher values than HSD.

The v_2 increase is clarified in Fig. 3 where the partonic fraction of the energy density at mid-pseudorapidity with respect to the total energy density in the same pseudorapidity interval is shown. We recall that the repulsive scalar mean field potential $U_s(\rho_s)$ for partons in the PHSD model leads to an increase of the flow v_2 as compared to that for HSD or PHSD calculations without partonic mean fields [21]. As follows from Fig. 3, the energy fraction of the partons substantially grows with increasing bombarding energy while the duration of the partonic phase is roughly the same. Accordingly, the increasing influence of the repulsive partonic mean-field $U_s(\rho_s)$ leads to an increase of the flow v_2 with bombarding energy. We point out that the increase of v_2 in PHSD relative to

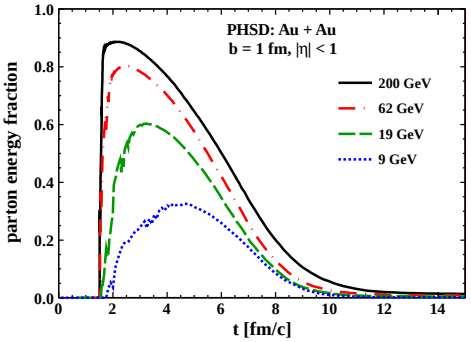


FIG. 3: The evolution of the parton fraction of the total energy density at the mid-pseudorapidity for different collision energies.

HSD is also partly due to the higher interaction rates in the partonic medium because of a lower ratio of η/s for partonic degrees of freedom at energy densities above the critical energy density than for hadronic media below the critical energy density [32, 33]. The relative increase in v_3 and v_4 in PHSD essentially is due to the higher partonic interaction rate and, thus, to a lower ratio η/s in the partonic medium, which is mandatory to convert initial spacial anisotropies to final anisotropies in momentum space [34].

Conclusions. The anisotropic flows – elliptic v_2, triangular v_3, and hexadecupole v_4 – are reasonably described within the PHSD model in the whole transient energy range naturally connecting the hadronic processes at moderate bombarding energies with ultrarelativistic collisions at RHIC energies where the quark-gluon DOF become dominant due to a growing number of partons. The smooth growth of the elliptic flow with collision energy demonstrates the increasing importance of partonic DOF This feature is reproduced by neither explicit hadronic kinetic models like HSD or UrQMD nor the AMPT model treating the partonic phase on the basis of pQCD with massless partons and a noninteracting equation-of-state for the partons. Further signatures of the transverse collective flow, the higher-order harmonics of the transverse anisotropy v_3 and v_4 change only weakly from $\sqrt{s_{NN}} \approx 7$ GeV to the top RHIC energy $\sqrt{s_{NN}} =$ 200 GeV, roughly in agreement with preliminary experimental data. Certainly, new measurements within the BES program at RHIC, especially for higher-order harmonics, will further constrain the partonic dynamics.

Acknowledgements. We are thankful to S. Voloshin for constructive remarks and O. Linnyk for useful discussions. This work has been supported in part by the DFG Grant WA 431/8-1, the DFG Grant CA 124/7-1, the RFFI Grants 08-02-01003-a, the Ukrainian-RFFI Grant 09-02-90423-ukr-f-a, and the LOEWE center HIC for FAIR.

[1] U. Heinz and M. Jacob, nucl-th/0002042.
[2] C. Alt *et al.* (NA49 Collaboration), Phys. Rev. **C77**, 024903 (2008); M. Gazdzicki, M. Gorenstein and P. Seyboth, Acta Phys. Polon. **B42**, 307 (2011).
[3] J.-Y. Ollitrault, Phys. Rev. **D46**, 229 (1992).
[4] U. Heinz and P. Kolb, Nucl. Phys. **A702**, 269 (2002).
[5] E. Shuryak, Prog. Part. Nucl. Phys. **62**, 48 (2009).
[6] H. Petersen, M. Bleicher, Phys. Rev. **C81**, 044906 (2010); H. Petersen, G.-Y. Qin, S. A. Bass, B. Müller, Phys. Rev. **C82**, 041901 (2010); G.-Y. Qin, H. Petersen, S. A. Bass, B. Müller, Phys. Rev. **C82**, 064903 (2010).
[7] E. V. Shuryak, Nucl. Phys. **A750**, 64 (2005).
[8] M. Gyulassy and L. McLerran, Nucl. Phys. **A750**, 30 (2005).
[9] A. Peshier and W. Cassing, Phys. Rev. Lett. **94**, 172301 (2005).
[10] C. Pruneau, S. Gavin and S. Voloshin, Nucl. Phys. **A715**, 661 (2003).
[11] R. A. Lacey *et al.*, Phys. Rev. Lett. **98**, 092301 (2007).
[12] R. S. Bhalerao *et al.*, Phys. Lett. **B627**, 49 (2005).
[13] B. Alver and G. Roland, Phys. Rev. **C81**, 054905 (2010).
[14] J. Xu and C. M. Ko, Phys. Rev. **C83**, 021903 (2011).
[15] K. Aamodt *et al.* (ALLICE Collaboration), Phys. Rev. Lett. **105**, 252302 (2010).
[16] G. Odyniec, Acta Phys. Polon. **B40**, 1237 (2009); B. I. Abelev *et al.* (STAR Collaboration), Phys. Rev. **C81**, 024911 (2010).
[17] M. M. Aggarwal *et al.* (STAR Collaboration), arXiv: 1007.2613 [nucl-ex].
[18] W. Cassing and E. L. Bratkovskaya, Nucl. Phys. **A831**, 215 (2009).
[19] W. Cassing, Nucl. Phys. **A791**, 365 (2007).
[20] W. Cassing, Nucl. Phys. **A795**, 70 (2007).
[21] E. L. Bratkovskaya *et al.*, Nucl. Phys. **A856**, 162 (2011).
[22] Y. Aoki *et al.*, JHEP **0906**, 088 (2009).
[23] W. Ehehalt and W. Cassing, Nucl.Phys.**A602**,449(1996).
[24] W. Cassing and E. L. Bratkovskaya, Phys. Rep. **308**, 65 (1999).
[25] H.-U. Bengtsson and T. Sjöstrand, Comp. Phys. Commun. **46**, 43 (1987).
[26] A. Bilandzic, R. Snellings and S. Voloshin, Phys. Rev. **C83**, 044913 (2011).
[27] M. Nasim, L. Kumar, P. K. Netrakanti and B. Mohanty, Phys. Rev. **C82**, 054908 (2010).
[28] X. -Y. Gong (PHENIX Collaboration), J. Phys. G **38**, 124146 (2011).
[29] E. L. Bratkovskaya, *et al.*, Phys. Rev. **C69**, 054907 (2004); Phys. Rev. Lett., **92**, 032302 (2004).
[30] S. A. Bass *et al.*, Prog. Part. Nucl. Phys. **41**, 255 (1998); M. Bleicher *et al.*, J. Phys. **G 25**, 1859 (1999).
[31] Z.-W. Lin and C. M. Ko, Phys. Rev. **C65**, 034904 (2002); Z.-W. Lin *et al.*, Phys. Rev. **C72**, 064901 (2005).
[32] S. Mattiello and W. Cassing, Eur. Phys. J. **C70**, 243 (2010).
[33] N. Demir and S. A. Bass, Phys. Rev. Lett. **102**, 172302 (2009).
[34] H. Petersen, C. Coleman-Smith, S. A. Bass, and R. Wolpert, J. Phys. **G38**, 045102 (2011).